1034
doi:10.1017/S1431927622004433
Microsc. Microanal. 28 (Suppl 1), 2022

Stability Range of Ti-Zr Alloy for Dental Implants

Nestor Florido-Suarez[1], Iosif Hulka[1], Julia Mirza-Rosca[1*], Adriana Saceleanu[2]

[1.] University of Las Palmas de Gran Canaria, Mechanical Engineering Department., University Campus of Tafira, Engineering Building, 35017 Las Palmas de Gran Canaria, Spain
[2.] "Lucian Blaga"University of Sibiu, Medicine Faculty, 550024 Sibiu, Romania
[*] Corresponding author: julia.mirza@ulpgc.es

1. INTRODUCTION

Even some of the first efforts at dental implants can be traced back to the antiquity period, the main developments in implant dentistry happened after 1700s and 1800s. Dentists and physicians started experimenting with gold and other metallic materials to provide support for false teeth. These early efforts were not successful, as the body tended to reject these first implants [1]. Taking into account that the binary Ti-Zr system exhibits complete solid solution, the aim of this research is to provide a correlation between the microstructure, microhardness and electrochemical properties of Ti-20Zr in artificial extracellular conditions for dental implants and the efforts were directed to finding an adequate range for the stability of this alloy and to evaluate the performance of the passive layers grown on it.

2. EXPERIMENTAL

The studied Ti-20Zr alloy, consisting of 80% titanium and 20% zirconium, (fabricated by R&D CS Bucharest, Romania - Research &Development Consulting and Services) was produced by vacuum melting. The samples were prepared from sponge Ti and Zr, both of them with more than 99.5mass% purity and to avoid differences in the macroscopic composition due to inadequate stirring, the ingots have been flipped and remelted a minimum of six times. The samples were held for 1 hour at 1000ºC and then air cooled.
The metallographic preparation [2,3] employed for titanium alloy specimens involves grinding to 1200 grit with SiC, followed by polishing with 0.3 μm alpha-alumina to a mirror finish. Samples are ultrasonically cleaned using purified water, and then etched in Kroll's etchant which contains HF, HNO3 and water for an immersion time of 20 seconds. An Olympus PME 3-ADL microscope was used for microscopic examinations.
The electrochemical behavior of the Ti-20Zr alloy in simulated physiological environment was evaluated by electrochemical impedance spectroscopy (EIS). Electrochemical determinations were performed at 25°C using a single compartment cell containing 75 ml of Ringer's solution (see Table1).

Table 1. Composition of Ringer Grifols solution

Compound	Composition (mmol/L)
Cl^-	111.5
Na^+	130
K^+	5.5
Ca^{2+}	1.7
$C_3H_5O_3^-$	27.2

The potential of the studied alloy was determined against a NaCl (saturated) - calomel electrode (SSCE) and the potentials reported were referenced to this electrode. A Pt cylindrical grid was employed as a counter electrode. AC impedance data were collected at various potentials [4] employing a PAR 263 A potentiostat coupled to a PAR 5210 lock-in amplifier. The AC potential range was fixed at 10 mV and single sine wave readings were made at frequencies in the range of 10-1 and 105 Hz.

3. RESULTS AND DISCUSSION

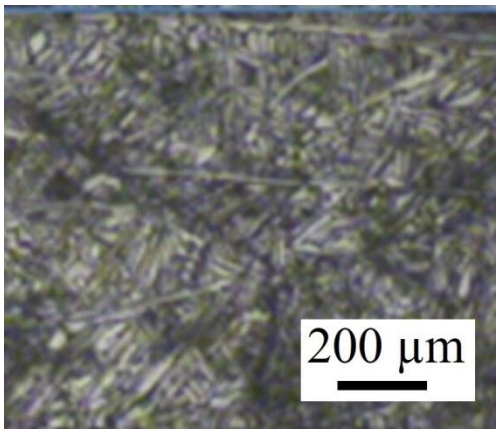

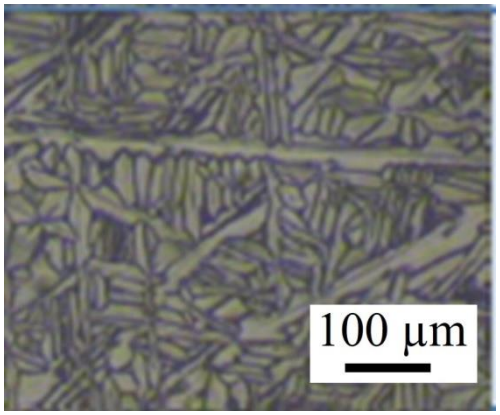

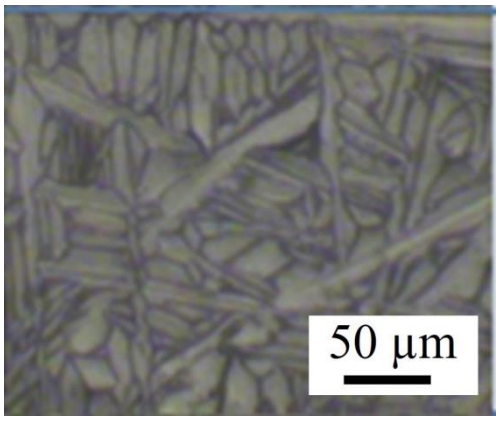

https://doi.org/10.1017/S1431927622004433 Published online by Cambridge University Press

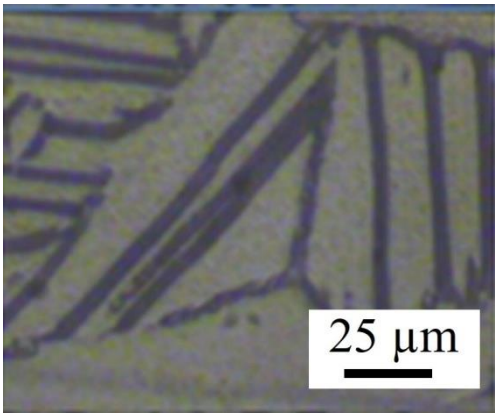

Fig. 1. Microscopical aspects of the surfaces, 15 seconds of etching at various magnifications

The microstructure of Ti-20Zr (see Fig.1) is greatly affected by the treatment background and heat processing; in this case, the material was kept for one hour at 1000°C, above β transus (the transformation temperature from α to all β) and cooled with air. A lamellar pattern with platelet α (light) and intergranular β (dark) is observed [5].

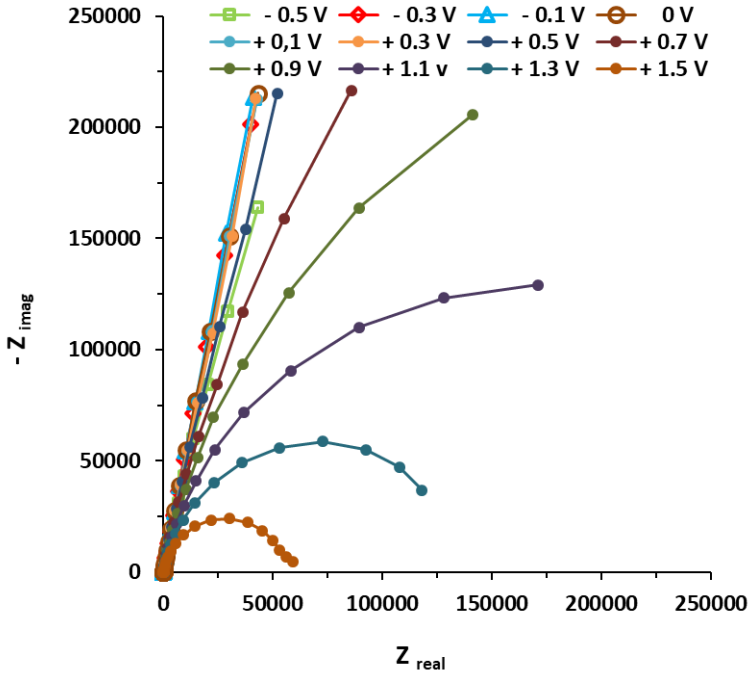

Fig.2. Nyquist curves of Ti-20Zr at different potentials

https://doi.org/10.1017/S1431927622004433 Published online by Cambridge University Press

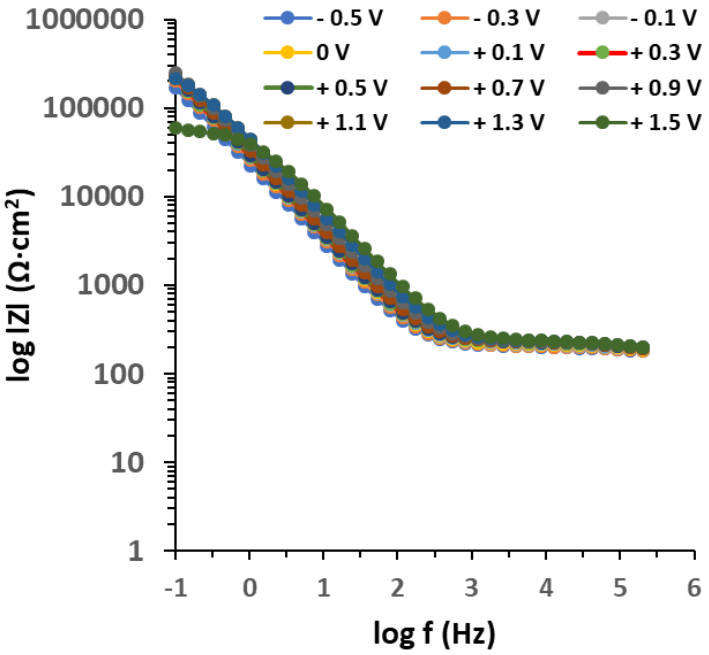

Fig.3. Bode-IZI for Ti-20Zr at different potentials

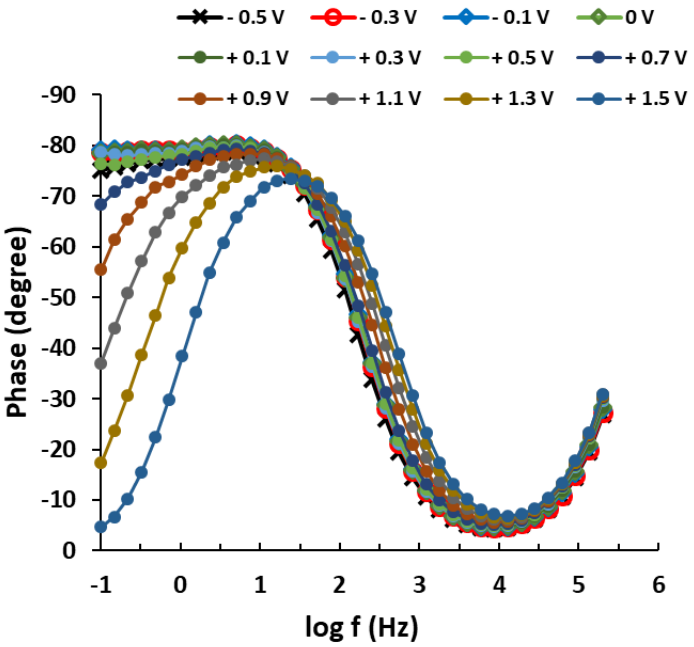

Fig.4. Bode-phase for Ti-20Zr at different potentials

The Nyquist plots (Fig.2) and Bode plots (Fig.3 and Fig.4) correspond to the impedance of Ti–20Zr at different potential values. Even the EIS data were recorded within the -0.5V and 1.5V vs. SCE potential range with a step of 200 mV, some of the obtained curves superposed each other as can be seen in the corresponding figures.

https://doi.org/10.1017/S1431927622004433 Published online by Cambridge University Press

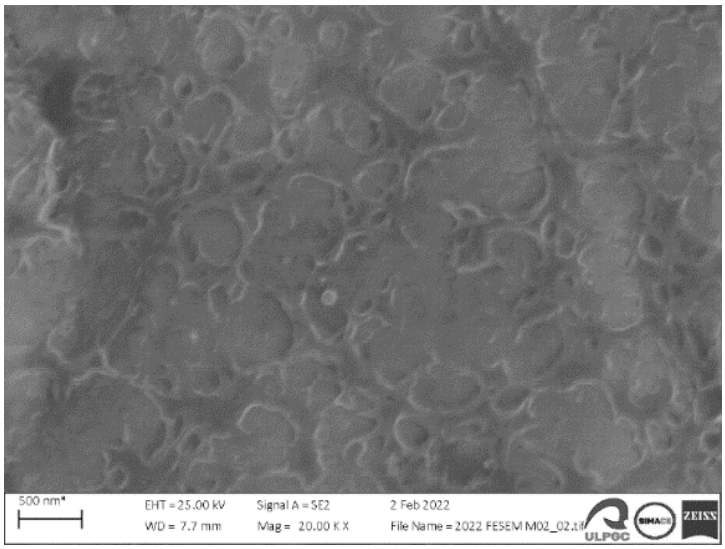

Fig.5. Surface topography taken with SE-detector on Ti-20Zr corroded sample.

Fig.5 presents the surface topography of Ti-20Zr alloy and it reveals the influence of simulated body fluid on the surface of the sample. Can be seen that the passive layer has an external porous film [7,8] which is suitable for oseoinduction growth of the bone.

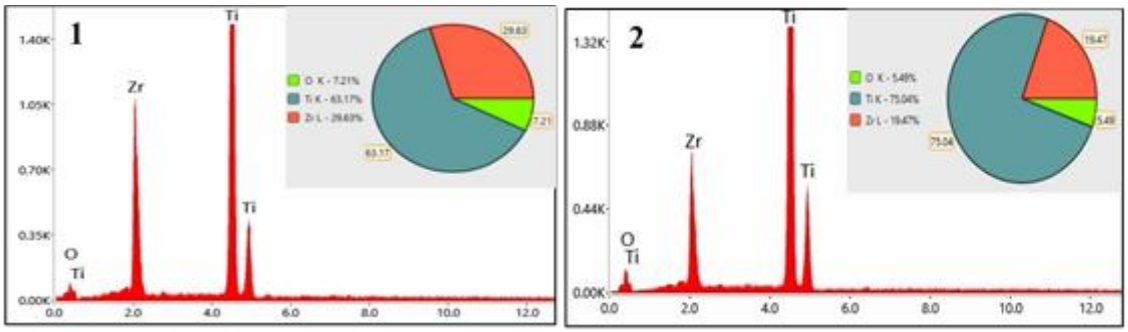

Fig. 6. Microstructure of Ti-20Zr alloy taken with BSD detector and EDX spectra with quantification

https://doi.org/10.1017/S1431927622004433 Published online by Cambridge University Press

In the wide range of low and medium frequencies, the spectra show a linear slope of approximately –1 in log |Z| as the frequency decreases [6], while the phase angle values are close to 80º(Fig.4). This is the typical response of a compact passive film capacitor.
At all potentials, a near capacitive response was detected, characterized in Nyquist plots (see Figure 2) by incomplete semicircles. In the higher frequency band (1–100 kHz), the Bode plot (Figure 3) shows constant values (horizontal line) of log |Z| versus log(f) with a phase angle approaching 0o.
It can be seen from the BSD micrograph (Fig.6) that the investigated area presents some dark gray and brighter regions. In SEM investigations with a BSD detector, the higher the atomic number, the more brilliant the material looks in the micrographs. These bright regions correspond to the Zr range zones. Zr atoms have a higher atomic number, so they scatter more electrons in the direction of the detector than Ti atoms and consequently appear more brilliant in the SEM micrographs. This is also confirmed by the EDX spectra, where the Zr peak is higher when collected in the bright area.

4. CONCLUSIONS

The α + β microstructure achieved by aging at 1273 K for one hour presents an improved mechanical biocompatibility, making it more appropriate compared to the other microstructures for dental implant applications. The Ti-20Zr alloy presents excellent corrosion resistance, superior to that of cpTi, and considering that there is a general consensus that Zr alloys do not have local or systemic toxic reactions, we can conclude that Ti-20Zr might be a promising biomaterial for employment as a dental implant [9].

REFERENCES

[1] Manam NS, Harun WSW, Shri DNA, Ghani SAC, Kurniawan T, Ismail MH, et al. Study of corrosion in biocompatible metals for implants : A review. J Alloys Compd 2017;701:698–715. https://doi.org/10.1016/j.jallcom.2017.01.196.
[2] ASTM E3-11(2017), Standard Guide for Preparation of Metallographic Specimens, ASTM International, West Conshohocken, PA, 2017 2017.
[3] Garcia-Falcon CM, Gil-Lopez T, Verdu-Vazquez A, Mirza-Rosca JC. Electrochemical characterization of some cobalt base alloys in Ringer solution. Mater Chem Phys 2021. https://doi.org/10.1016/j.matchemphys.2020.124164.
[4] Socorro-Perdomo PP, Florido-Suárez NR, Mirza-Rosca JC, Saceleanu MV. EIS Characterization of Ti Alloys in Relation to Alloying Additions of Ta. Materials (Basel) 2022;15. https://doi.org/10.3390/ma15020476.
[5] Ibriş N, Mirza Rosca JC. EIS study of Ti and its alloys in biological media. J Electroanal Chem 2002;526:53–62. https://doi.org/10.1016/S0022-0728(02)00814-8.
[6] Perdomo-Socorro PP, Florido-Suárez NR, Verdú-Vázquez A, Mirza-Rosca JC. Comparative EIS study of titanium-based materials in high corrosive environments. Int J Surf Sci Eng 2021;15:152–64. https://doi.org/10.1504/IJSURFSE.2021.116333.
[7] González JEG, Mirza-Rosca JC. Study of the corrosion behavior of titanium and some of its alloys for biomedical and dental implant applications. J Electroanal Chem 1999;471:109–15. https://doi.org/10.1016/S0022-0728(99)00260-0.
[8] Izquierdo J, Mareci D, Bolat G, Santana JJ, Rodríguez-Raposo R, Fernández-Mérida LC, et al. Improvement of the corrosion resistance of biomedical zr-ti alloys using a thermal oxidation treatment. Metals (Basel) 2020;10. https://doi.org/10.3390/met10020166.
[9] The authors acknowledge the structural founds project CABINFR2019-07 for providing the infrastructure used in this work.